

Ageing and Quenching: Influence of Galaxy Environment and Nuclear Activity in Transition Stage

Pius Privatus^{a,1,2,*} and Umananda Dev Goswami^{b,1,‡}

¹*Department of Physics, Dibrugarh University, Dibrugarh 786004, Assam, India*

²*Department of Natural Sciences, Mbeya University of Science and Technology, Iyunga 53119, Mbeya, Tanzania*

This study aims to investigate whether the environment and the nuclear activity of a particular galaxy influence the ageing and quenching at the transition stage of the galaxy evolution using the volume-limited sample constructed from the twelve release of the Sloan Digital Sky Survey. To this end, the galaxies were classified into isolated and non-isolated environments and then each subsample was further classified according to their nuclear activity using the WHAN diagnostic diagram, and ageing diagram to obtain ageing and quenching galaxies. The ageing and quenching galaxies at the transition stage were selected for the rest of the analysis. Using the star formation rate and the $u-r$ colour-stellar mass diagrams, the study revealed a significant change of 0.03 dex in slope and 0.30 dex in intercept for ageing galaxies and an insignificant change of 0.02 dex in slope and 0.12 dex in intercept of the star formation main sequence between isolated and non-isolated quenching galaxies. Further, a more significant change in the number of ageing galaxies above, within and below the main sequence and the green valley was observed. On the other hand, an insignificant change in the number of quenching galaxies above, within and below the main sequence and the green valley was observed. The study concludes that ageing depends on the environment and the dependence is influenced by the nuclear activity of a particular galaxy while quenching does not depend on the environment and this independence is not influenced by the nuclear activity.

Keywords: Ageing; Quenching; Main sequence; Green valley; Galaxy environment.

I. INTRODUCTION

The processes of galaxy evolution and the end of star formation within the galaxy remain in hot debate to date, with unsolved issues including the role of the environment and the nature of the feedback mechanism. This is due to the complex nature of the physical processes underlying this field, despite the fact that the relation between the star formation history (SFH) of galaxies and their physical properties such as stellar mass, environment, morphology and chemical composition has been extensively studied during the last few decades [1–3]. The distribution of most of the galaxy’s physical properties including star formation rate (SFR), stellar mass (M_\star) and colour have been proven to be bimodal, e.g. in Refs. [3, 4] the galaxies are classified into star forming with abundant gas reservoirs and passive that correspond to gas-poor [5, 6]. Due to such bimodal distributions of properties, the galaxies are divided with respect to the main sequence (MS, having a tight correlation between SFR and M_\star) into within (normal star forming), above (starburst) and below (passive) the MS, where the starburst are galaxies that undergo excess star formation activity and the passive have little star formation activity [7–15]. The star forming was observed to be in the blue cloud (BC), while the retired galaxies were in red sequence (RS). The galaxies in intermediate were defined to be in the green valley (GV) in colour against M_\star diagrams [16–18].

In recent years different internal and external (environmental) processes have been proposed as the main reason for the transition from the BC to the RS mostly characterised by the decrease in SFR referred to as quenching and ageing. Quenching has been defined as a mechanism able to terminate the star formation process in a galaxy by an agent (e.g. negative feedback from Active Galactic Nuclei (AGN) or supernovae winds) which causes either the removal or heating of the cold gases necessary for star formation, while the term ageing denotes the continuous evolution of a galaxy through a secular process driven by the life cycle of its stars [19, 20]. For the internal processes the galaxy may quench due to internally triggered quenching mechanisms such as negative feedback from AGN, supernovae winds or the stabilisation of the gas against fragmentation [21, 22]. On the other hand, external processes triggered quenching may be due to environmentally driven processes such as ram pressure stripping able to remove the gas reservoir, strangulation or starvation (leading to the suppression of gas infall or galaxy interactions) [23, 24]. These processes are observed to slow down the rate of star formation but also enhance the star formation in a short time scale [25]. Quenching has been categorised into fast and slow quenching depending on the duration of time spent to cross an arbitrary boundary in the M_\star versus specific star formation rate ($\text{SSFR} = \text{SFR}/M_\star$) plane and colour-magnitude diagram [26–28]. The fast quenching involves the termination of SFR in a short time scale that is less than 1 Gyr and slow quenching involves the termination of SFR with a time scale comparable to the age of the universe. In this regard ageing is different but difficult to distinguish from slow quenching, they significantly differ in the fact that quenching involve agents and

^b Corresponding author

* Email: privatuspius08@gmail.com

‡ Email: umananda@dibru.ac.in

active suppression of star formation while ageing does not, more important to keep in mind is that both processes results in the transition of galaxies from BC to RS [19, 20].

Ref. [29] studied the radial profiles of emission lines from galaxies to quantify the $H\alpha$ emission line strength in a galaxy's spectrum relative to its continuum emission ($H\alpha$ equivalent width, denoted as $EW(H\alpha)$) and SSFR derived from spatially resolved Mapping Nearby Galaxies at Apache Point Observatory (MaNGA) survey as detailed in Ref. [30], to gain insight into the physical mechanisms that suppress the star formation, and observed that the responsible quenching mechanism appears to affect the entire galaxy. Ref. [31] obtained that morphology and environment have a combined role in slowing down the star formation activities in galaxies. Furthermore, they observed that a long-timescale environmental effect appears at low redshift. It needs to be mentioned that our current study specifically focuses on the effects of environment and nuclear activity on the galaxies' star formation activities, keeping the morphology effect as a future prospect of a detailed study. Ref. [32] suggested that the decrease of SFR is mainly due to internal process and is linked with bulge growth. However, the existence of the relation between the morphology and density may lead to a change in the relation of SFR, stellar mass and the environment where a particular galaxy resides. The study by Ref. [33], presenting the analysis of star formation and quenching in the SDSS MaNGA survey as detailed in Ref. [30], utilising over 5 million spaxels from ~ 3500 local galaxies observed that the sudden decrease of SFR affect the whole galaxy but star formation occurs in a small localised scale within the galaxy. On the other hand Ref. [33] observed that quenching is global while star formation is governed by local processes within each pixel. All these studies aim to discern the mechanism or combination of mechanisms that lead to the quenching of star formation processes in galaxies, thereby influencing their evolution.

In a simplified representation, as already stated the processes guiding the galaxy transformations can be broadly categorised as internal and external mechanisms. Processes like negative feedback from AGN, supernovae winds act within the galaxy and are classified under internal mechanisms, while processes like ram-pressure stripping and galaxy mergers originate from the external mechanisms. The study by Ref. [8], pointed out that correlation between SFR and M_\star decreases with redshift ($\propto (1+z)^\gamma$, where γ ranges from 1.9 to 3.7) rather than being driven solely by stochastic events like major mergers or starbursts [34–36]. On the other hand, the study by Ref. [37] using the semi-analytic model of galaxy formation, observed that the AGN feedback is the primary mechanism affecting the quenching. Although this was observed to affect the massive galaxies (with $M_\star \geq 10^{11} M_\odot$), hence there is a lack of observed feedback effects for the majority of the star forming galaxies [38]. However, Ref. [39] using a basic model for disk evolution, demonstrated that the evolution of galaxies away from the main sequence can be attributed to the depletion of gas due to star formation after a cut-off of gas inflow. This model was based on the observed dependence of star formation on gas content in local galaxies and assuming simple histories of cold gas inflow. Again Ref. [39] using the MS as the tracer of the factors responsible for quenching further obtained that galaxies classified as MS, quiescent (with reduced star formation), or passive (with no ongoing star formation) exhibit varying fractions on mass and environment. The MS fractions decrease with increasing mass and density, while the quiescent and passive fractions rise. Due to this uncertainty, the ongoing debate revolves around the extent to which each of these scenarios influences the shape of the relationship.

By examining the physical characteristics of MaNGA as detailed in Ref. [30] and the Sydney-Australian Astronomical Observatory (AAO) Multi-object Integral field spectrograph (SAMI) Galaxy Survey as detailed in Refs. [40, 41], Ref. [20] found that the ageing population is made up of a heterogeneous mixture of galaxies, primarily late-type systems (e.g. spiral and irregular galaxies), since they start with high SFR, as they becomes older their SFR decreases results to the transition from star-forming (high SFR) to quiescent states (reduced SFR) with a range of physical features. Authors pointed out that the retired (galaxy systems that have ceased star formation) were formerly ageing or quenched. These galaxies are found across different masses and environments ranging from low-mass ($M_\star < 10^{11} M_\odot$), low-density ($\Sigma_5 < 1 \text{ Mpc}^{-2}$) regions to high-mass ($M_\star \geq 10^{11} M_\odot$), high-density ($\Sigma_5 \geq 1 \text{ Mpc}^{-2}$) ones, where Σ_5 is the surface density of galaxies to the 5th nearest neighbour given by $\Sigma_5 = 5/\pi d_5^2$. Here d_5 is the projected distance to the 5th nearest neighbouring galaxy, measured in Mpc. In their analysis they shows that distinguishing between retired and recently quenched galaxies are important to constrain the mechanisms driving galaxy evolution. They further left two questions viz., whether galaxies evolve due to their initial conditions at formation such as chemical composition, the angular momentum, mass of the galaxy and the initial density of environment (nature)? Or the external quenching mechanism such as the environment, galaxy interactions and AGN feedback (nurture)? Distinguishing between these factors is very important in understanding galaxy transformation.

As the follow-up of the work by Ref. [20], this study aims to investigate whether the environment influences ageing and quenching, and how their relationships with the environment are affected by nuclear activity. This study uses the friends-of-friend method from Ref. [42], to assign ageing and quenching galaxies in a transition stage into systems of isolated (with no neighbour) and non-isolated (with at least one neighbour) environment and then to compare their equations of the main sequence, the colour obtained from u - and r -band luminosities ($u - r$ colour) and stellar mass diagrams.

Our paper is organized as follows. In the next section, we explain the source of data and the method of getting samples. In Section III we explain the methodology used in this study. The Section IV is dedicated to presenting the results. In Section V the results are discussed. Section VI presents the summary and conclusion. Cosmological constants used in this work are adopted from Ref. [43], wherein the dark energy density parameter $\Omega_\Lambda = 0.692$, Hubble constant $H_0 = 67.8 \text{ km s}^{-1} \text{ Mpc}^{-1}$ and the matter density parameter $\Omega_m = 0.308$ are recorded.

II. DATA

A. The SDSS main sample

In this research work the catalogue data extracted from the flux-limited sample of twelve releases of Sloan Digital Sky Survey (SDSS DR12) as detailed in Ref. [44, 45] are used. The main galaxy sample was selected from the main contiguous area of the survey based on the methods outlined in Ref. [42]. Galaxy data were downloaded from the SDSS Catalogue Archive Server (CAS). The objects with the spectroscopic class GALAXY or QSO as detailed in Ref. [45], were selected as suggested by the SDSS team. We then filtered out galaxies with the galactic-extinction-correction based on Ref. [46] where Petrosian r-band magnitude fainter than 17.77 are rejected keeping in mind that the SDSS is incomplete at fainter magnitudes [47]. After correcting the redshift for the motion with respect to the cosmic microwave background (CMB), using the simplified formula $z_{\text{CMB}} = z_{\text{obs}} - v_p/c$, where v_p is a velocity of motion along the line of sight relative to the CMB, the upper distance limit at $z = 0.2$ was set. The final data set contains 584449 galaxies.

B. The volume-limited samples

As already stated the SDSS main data are flux-limited, one of the disadvantages of using the flux-limited sample is that only the luminous objects have a chance to be observed at large distances. Due to this main reason, the volume-limited samples are desired. Hence we constructed a volume-limited sample for uniformity. Due to the peculiar velocities of galaxies in groups, the measured redshift (recession velocity) does not give an accurate distance to a galaxy located in a group or cluster, the apparent magnitude was transformed into absolute magnitude using the relation:

$$M_r = m_r - 25 - 5 \log_{10}(d_L) - K, \quad (1)$$

where d_L is the luminosity distance, M_r and m_r are r-band absolute and apparent magnitudes respectively, and K is the k+e-correction. The k-corrections were calculated with the KCORRECT (*v4.2*) algorithm [48]. The evolution corrections were estimated using the luminosity evolution model of $K_e = c * z$, where $c = -4.22, -2.04, -1.62, -1.61, -0.76$ for the u,g,r,i,z-filters, respectively [49]. The magnitudes corresponding to the rest frame (at the redshift $z = 0$) and evolution correction were estimated similarly by assuming a distance-independent luminosity function [50, 51]. According to Ref. [52], the Schechter function's [53] typical magnitude M_r^* is around -20.5 mag. The physical properties of galaxies have been shown to undergo an abrupt transition at the typical magnitude M_r^* . Clustering depends weakly on the environment for galaxies fainter than M_r^* but is stronger for brighter galaxies [54]. We have constructed the volume-limited samples above the characteristic magnitude M_r^* by calculating the effective maximum distance using the relation as given by

$$d_{\text{max}} = 10^{(m_{r\text{lim}} - M_{r\text{min}} + 5)/5} \times 10^{-6} (\text{Mpc}), \quad (2)$$

where $m_{r\text{lim}} = 17.17$ mag, $M_{r\text{min}} = -20.5$ mag. Using the d_{max} values and the luminosity restrictions we constructed the volume-limited main galaxy sample containing 136274 galaxies within $-22.5 \leq M_r \leq -20.5$ (mag).

III. METHODOLOGY

A. Isolated and non-isolated environments

Using the volume-limited sample defined in the previous section we assigned the galaxies into isolated and non-isolated sub-samples, compiled using the friend-of-friend (FoF) method with a variable linking length. The essence of this approach lies in the division of the sample into distinct systems through an objective and automated process. This involves creating spheres with a linking length (R) around each sample point (galaxies). The linking length was adjusted using the arctangent law as given by

$$R_{LL}(z) = R_{LL,0} \left[1 + a \arctan \left(\frac{z}{z_*} \right) \right], \quad (3)$$

where $R_{LL}(z)$ is the linking length used to create a sphere at a specific redshift, $R_{LL,0}$ is the linking length at $z = 0$, a and z_* are free parameters. We obtained the linking length (which defines a sphere used to group galaxies) by fitting the arctangent law defined by equation (3) to the observational data (nearest neighbour distance with redshift). The best-fit values for the parameters were: $R_{LL,0} = 0.34$ Mpc, $a = 1.4$ and $z_* = 0.09$ [42]. If there are other galaxies within the sphere, they are considered as the parts of the same system and referred to as “friends”. Subsequently, additional spheres are drawn around these newly identified

neighbours, and the process continues with the principle that “any friend of my friend is my friend”. This iterative procedure persists until no new neighbours or “friends” can be added. At that point, the process concludes, and a system is defined. The galaxies in the system with no neighbour ($N_{gal} = 1$) are isolated, while the galaxies with more than one neighbour ($N_{gal} \geq 2$) are non-isolated. Consequently, each system comprises an isolated galaxy or a non-isolated galaxy that shares at least one neighbour within a distance not exceeding R . A total of 58032 (42.59%) isolated and 78233 (57.41%) non-isolated galaxies were obtained.

B. Galaxy properties

The stellar masses used in this study were obtained from the MPA-JHU team and calculated from the Bayesian approach as detailed in Ref. [1]. Stellar mass calculation within the SDSS spectroscopic fiber aperture relies on the fiber magnitudes, whereas the total stellar mass is determined using the model magnitudes.

The MPA-JHU total SFR used in this study was derived from the MPA-JHU database and estimated using the methods of Refs. [2, 4] with adjustments made for non-star forming galaxies. The MPA-JHU team uses the $H\alpha$ calibration outlined in Ref. [55] to determine the SFR for galaxies classed as star forming. In contrast to the approach taken by Ref. [4], the MPA-JHU team applied aperture corrections for SFR by fitting the photometric data from the outer regions of the galaxies. Specifically, for SFR computation, Ref. [4] outlined the calculation within the galaxy fiber aperture. It is important to keep in mind that the region beyond the fiber SFR is estimated using the methods of Ref. [56]. Furthermore, for the case of AGN and weak emission line galaxies, SFR was determined using photometry. Keeping in mind that in the case of non-star forming galaxies, the ionisation originates from other sources, such as rejuvenation in the outer regions, post-AGB stars, or ionisation from AGN. As such, the SFR based on $H\alpha$ for non-star forming galaxies need to be regarded as a maximum value [57].

C. Galaxy classification

Intending to study where nuclear activity affects the dependence of ageing and quenching on environment, we classified the galaxies based on nuclear activity using the $W_{H\alpha}$ versus $[NII]/H\alpha$ (WHAN) diagram as detailed in Ref. [58], where $W_{H\alpha}$ is the $H\alpha$ equivalent width, and $[NII]/H\alpha$ is the ratio of the $[NII]$ emission line to the $H\alpha$ line. From this diagram we can have following four inequalities [58]:

$$\log \left(\frac{[NII]}{H\alpha} \right) < -0.4 \quad \text{and} \quad W_{H\alpha} > 3 \text{ \AA}, \quad (4)$$

$$\log \left(\frac{[NII]}{H\alpha} \right) > -0.4 \quad \text{and} \quad W_{H\alpha} > 6 \text{ \AA}, \quad (5)$$

$$\log \left(\frac{[NII]}{H\alpha} \right) > -0.4 \quad \text{and} \quad 3 \text{ \AA} < W_{H\alpha} < 6 \text{ \AA}, \quad (6)$$

$$W_{H\alpha} < 3 \text{ \AA}. \quad (7)$$

These inequalities (4), (5), (6), and (7) represent the pure star-forming (SF) galaxies, strong AGN, weak AGN and retired galaxies (RGs) respectively [58]. The use of the WHAN diagram is based on the fact that the usual traditional diagnostic diagrams detailed in Refs. [13, 59–61], may introduce bias since it is well-known that shock ionisation and AGNs could cover almost any region between the right-low end of the loci usually assigned to SF regions, up to the top-right end of the diagram. On the other hand low-ionisation nuclear emission-line region (LINER) may contain possible multiple ionising sources [58, 62–64]. The distributions of galaxies are shown in Fig. 1 wherein the SF galaxies are shown by blue colour, strong AGN by red colour, weak AGN by green colour and retired galaxies by cyan colour. The following numbers was obtained for isolated galaxies: 30261 ($\sim 52\%$) SF galaxies; 9582 ($\sim 17\%$) strong AGN; 3604 ($\sim 6\%$) weak AGN and 14585 ($\sim 25\%$) retired, while for the non-isolated sample: 31137 ($\sim 40\%$) SF galaxies; 10921 ($\sim 14\%$) strong AGN; 5320 ($\sim 7\%$) weak AGN and 30855 ($\sim 39\%$) retired.

We classified the galaxies into ageing and quenching systems using the ageing diagrams (ADs) as detailed in Ref. [19, 20], given by Eqs. (8) (ageing line) and (9) (quenching line) respectively. The galaxies located above ageing and quenching lines are classified as ageing galaxies (AGs) while the galaxies below ageing and quenching line are quenching galaxies (QGs). The galaxies below the quenching line and above the ageing line are retired while the ones above the quenching line and below the ageing line are undetermined. The ADs are shown in Fig. 2, whereby for isolated a total number of 41886 ($\sim 72\%$), 447 ($\sim 1\%$), 14869 ($\sim 26\%$), and 836 ($\sim 1\%$) were obtained respectively for AGs, QGs, retired and undetermined galaxies, while

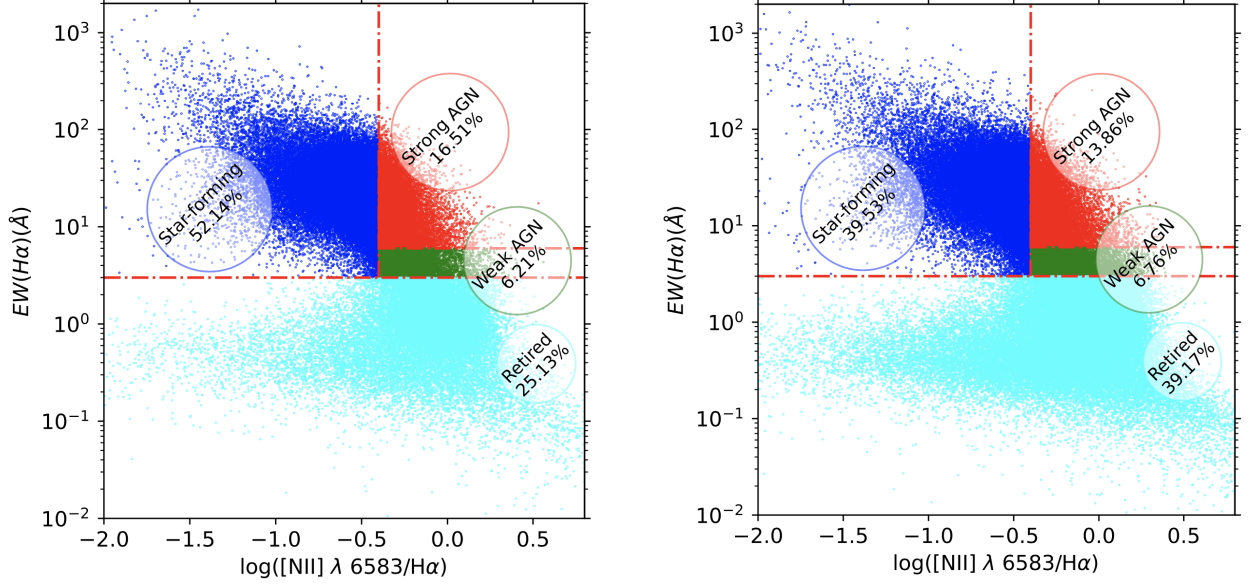


FIG. 1. The WHAN diagrams for the volume-limited main galaxy sample for isolated (left panel) and non-isolated (right panel) cases.

for non-isolated a total number of 46862 ($\sim 58\%$), 876 ($\sim 1\%$), 31066 ($\sim 40\%$), and 1001 ($\sim 1\%$) were obtained for AGs, QGs, retired and undetermined galaxies. It is very important to keep in mind that retired galaxies originate from both quenching and ageing processes, whereby the galaxies transit from blue cloud to red sequence. This transition is measured in terms of the colour index parameter ($g-r$) which is the difference between g (green)- and r (red)-band luminosities. The lower values of the colour index ($g-r \leq 0.5$) indicate that the galaxy is in a blue cloud, while its higher values ($g-r \geq 0.7$) indicate that the galaxy is in a red sequence. Since in this study our target is the galaxies in transition stage it is necessary to use the criteria between blue cloud and red sequence given by $0.5 < (g-r) < 0.7$, which implies that the galaxies are neither in blue cloud nor in red sequence. Keeping in mind that the associated uncertainties in measurements (e.g. sky background and noise) of g (green)- and r (red)-band luminosities may affect the classification, we minimized the uncertainty in the g -band using the same method used for the r -band luminosity through equation (1) as explained under Section II B. Moreover, we used the luminous galaxies to minimize the effect of noise. A total of 16929 and 16523 isolated and non-isolated ageing galaxies in transition (AGT) was obtained while a total of 133 and 286 isolated and non-isolated quenched galaxies in the transition stage (QGT) were obtained. We will use the AGT and QGT samples in the next sections unless otherwise stated.

$$\text{Ageing: } EW(H\alpha)/\text{\AA} = 250.0 \cdot 10^{-1.2 \cdot D_n(4000) - 4.3}, \quad (8)$$

$$\text{Quenched: } EW(H\alpha)/\text{\AA} = -12.0 \cdot 10^{-0.5 \cdot D_n(4000) + 1.8}. \quad (9)$$

IV. RESULTS

A. Ageing

The equations of the main sequence for SF galaxies show a tight relationship between the $\log(\text{SFR})$ and $\log(M_*)$, and the relation has been studied in a number of works [7–15]. The relationship serves as the tracer on how the stars are formed in relation to the stellar mass within a galaxy. Aiming at studying how the environment affects the SFR relative to the M_* for the ageing and quenching galaxies, and how the relations are affected by the nuclear activity, we generate the equation of the best-fitted line used to understand the behaviour of SFR relative to M_* for all galaxies residing in isolated and non-isolated environments. Fig. 3 shows the distributions of SFR with respect to M_* of the SF, strong AGN, and weak AGN galaxies for isolated and non-isolated cases along with the corresponding best-fitted MS line of the SF galaxies. The width of the MS of $\sim \pm 0.3$ dex (red dashed lines) in the plots of this figure is selected based on the dispersion of the observed MS. Table I indicates the percentage change between isolated and non-isolated galaxies above MS, within MS and below MS for SF (columns 2 and 3), Strong AGN (columns 4 and 5), Weak AGN (columns 6 and 7) galaxies, respectively.

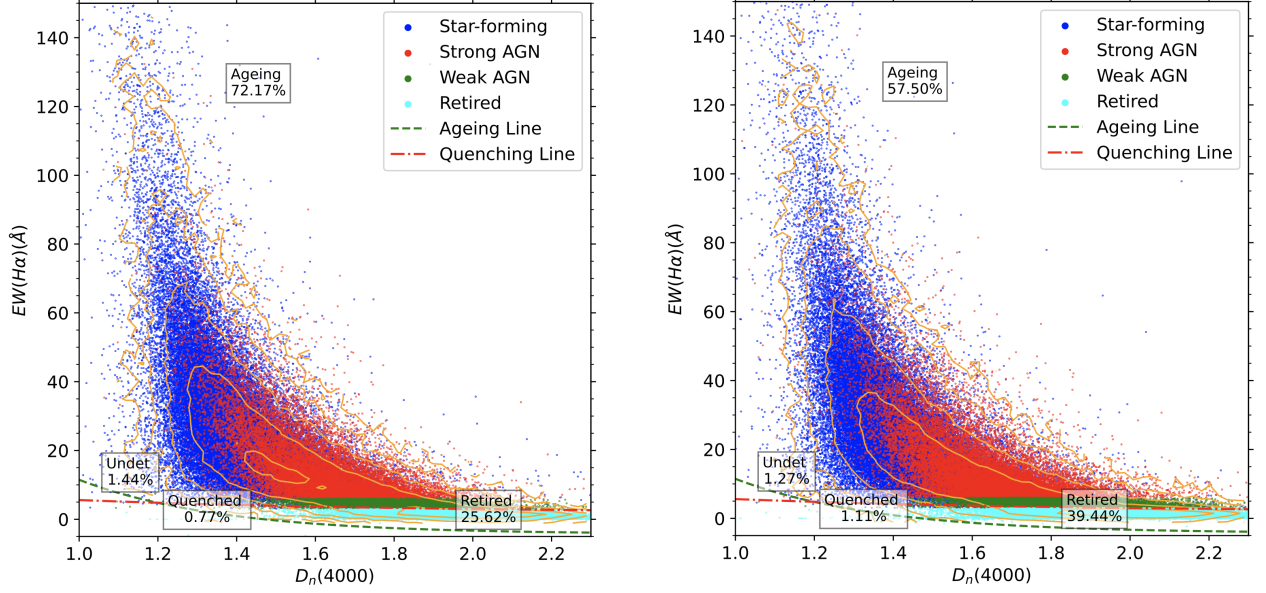


FIG. 2. Ageing diagrams (ADs) for the volume-limited main galaxy sample for isolated (left panel) and non-isolated (right panel) cases.

By performing the regression analysis for our samples, the general equations of the best-fitted line for the isolated and non-isolated galaxies are respectively given by

$$\log_{10}(\text{SFR}) = 0.60 \pm 0.01 \log_{10}(M_{\star}) - 5.99 \pm 0.14, \quad (10)$$

$$\log_{10}(\text{SFR}) = 0.63 \pm 0.01 \log_{10}(M_{\star}) - 6.28 \pm 0.14, \quad (11)$$

where the associated errors are standard deviations in the slope and intercept.

TABLE I. Number of galaxies within (MS), above (Above MS), and below (Below MS) the star-forming main sequence for the isolated (I) and non-isolated (NI) environments for the ageing transition (AGT) volume-limited sample.

Position (1)	Star-forming (%)		Strong AGN (%)		Weak AGN (%)	
	I (2)	NI (3)	I (4)	NI (5)	I (6)	NI (7)
MS	6525(78.04)	6242(78.53)	4709(67.68)	4754(67.75)	610(37.89)	577(37.06)
Above MS	958(11.46)	886(11.15)	782(11.24)	825(11.76)	1(0.06)	1(0.06)
Below MS	878(10.50)	821(10.33)	1467(21.08)	1438(20.49)	999(62.05)	979(62.88)
Total	8361(100)	7949(100)	6958(100)	7017(100)	1610(100)	1557(100)

Galaxies can be categorised further into two groups: those actively forming stars, appearing blue, and those lacking significant star formation, appearing red. The galaxies initially fall into the blue sub-category and then they change gradually to red [5, 6]. It is clear to say that evolution from one category to another must involve processes that quench their rate of forming new stars from the blue cloud passing the intermediate stage (green valley) to the red sequence [16, 17]. The factors for this transformation may be due to internal mechanisms like negative feedback from the AGNs and the galaxy environment. To study the effect of the environment on colour, Table II shows the number of galaxies with respect to the Green Valley (GV) for ageing galaxies. The position of galaxies on the colour against the stellar mass diagram is shown in Fig 4 for the SF, strong AGN, and weak AGN galaxies respectively. The width of the GV is derived following the criteria from Ref. [18], given by equations (12) and (13) representing the upper and lower lines, respectively as

$$u - r = -0.24 + 0.25 \times M_{\star}, \quad (12)$$

$$u - r = -0.75 + 0.25 \times M_{\star}. \quad (13)$$

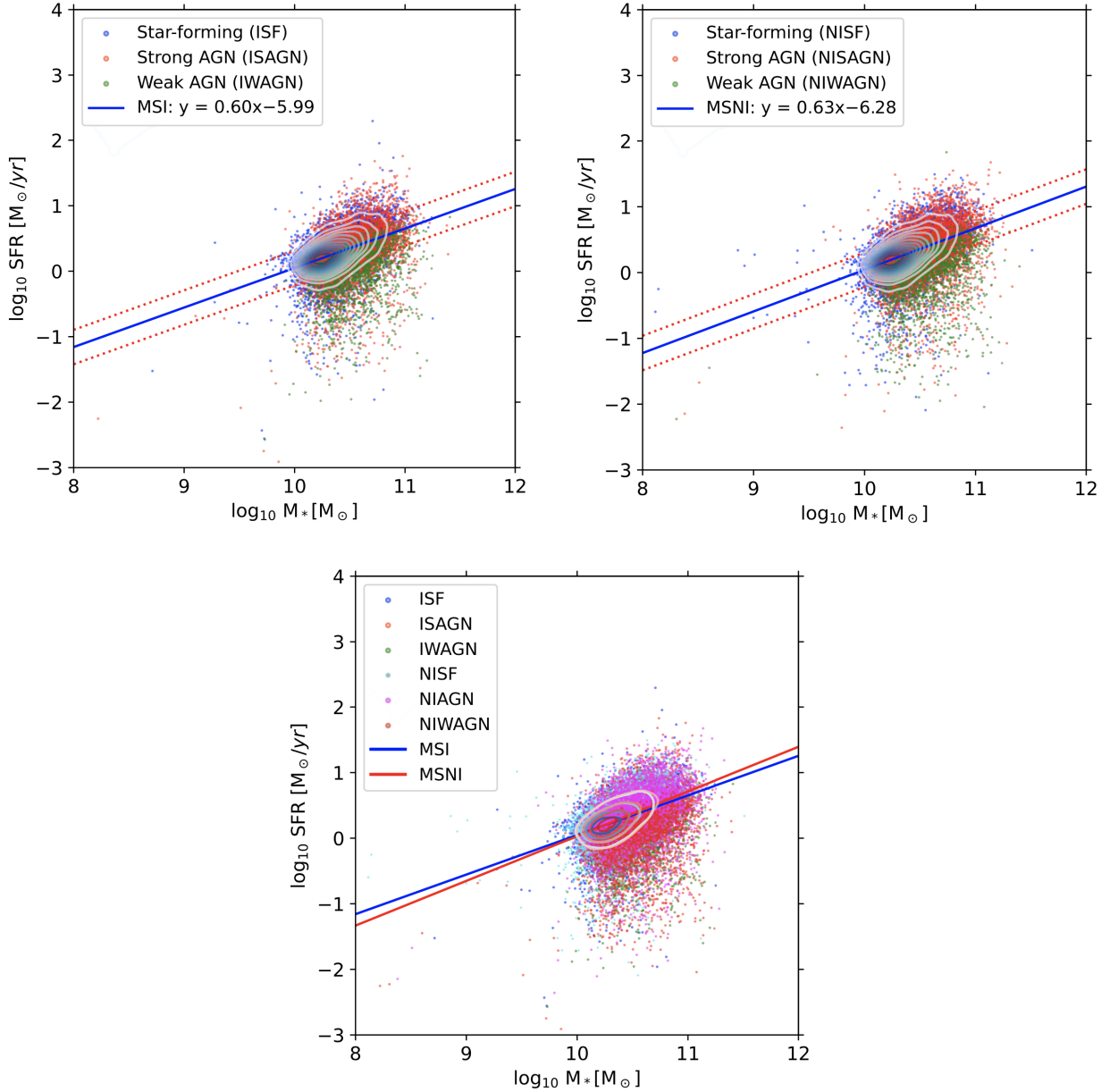


FIG. 3. Star formation main sequence (MS) for ageing galaxies: isolated sample (top left panel), non-isolated sample (top right panel), isolated and non-isolated on the same plot (bottom panel). In plots, MSI and MSNI denote the equations of the main sequence for isolated and non-isolated galaxies, respectively.

Here u and r magnitudes were derived from the SDSS database with extinction corrected. Table II indicates the positioning of galaxies with respect to the GV with its percentage for isolated and non-isolated galaxies for the ageing sample above GV, within GV and below GV for SF (columns 2 and 3), strong AGN (columns 4 and 5), weak AGN (columns 6 and 7) galaxies, respectively.

B. Quenching

As we have done in the previous subsection above, we do the same for the quenching galaxies. Fig. 5, shows the distributions of SFR with respect to M_* of the SF, strong AGN, and weak AGN galaxies for the isolated and non-isolated cases along with the corresponding best-fitted MS line of the SF for quenching galaxies. By performing regression analysis for our samples, the

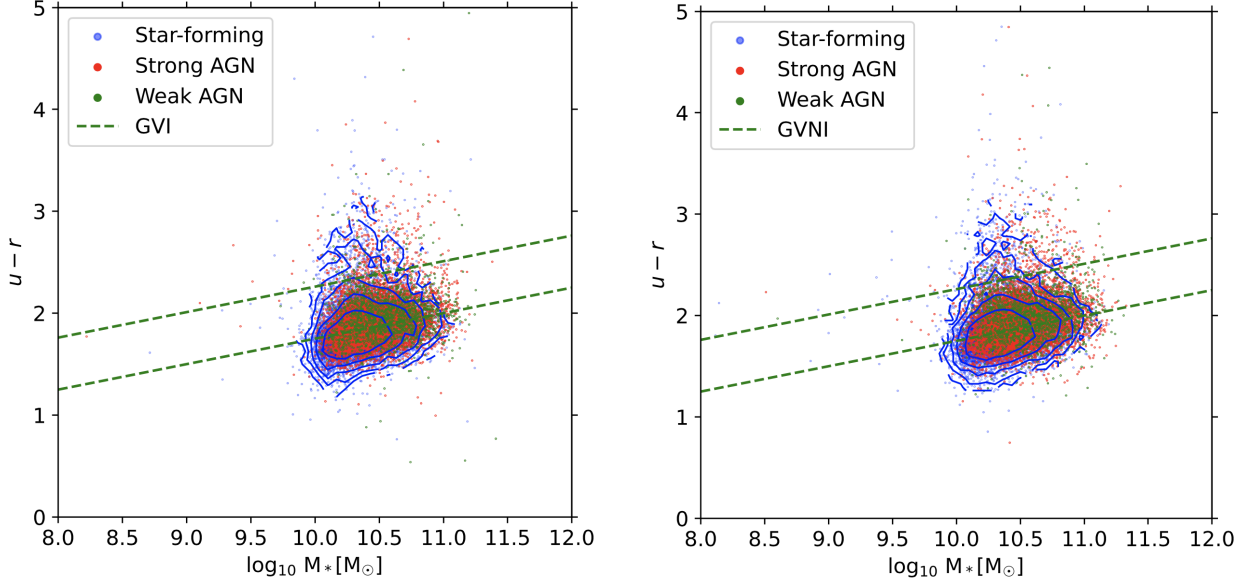


FIG. 4. Ageing galaxies' $u-r$ colour against stellar mass diagrams for isolated (left panel) and non-isolated (right panel) samples. Here, GVI and GVNI denote the green valleys for isolated and non-isolated galaxies, respectively.

TABLE II. Number of galaxies within the green valley (GV), above the green valley (Above GV) and below the green valley (Below GV) for isolated (I) and non-isolated (NI) galaxies for the ageing sample.

Position (1)	Star-forming (%)		Strong AGN (%)		Weak AGN (%)	
	I (2)	NI (3)	I (4)	NI (5)	I (6)	NI (7)
GV	3334(39.88)	3428(43.12)	3674(52.80)	3800(54.15)	920(57.14)	931(59.79)
Above GV	386(4.62)	424(5.33)	319(4.58)	340(4.85)	90(5.59)	96(6.17)
Below GV	4641(55.51)	4097(51.54)	2965(42.61)	2877(41.00)	600(37.27)	530(34.04)
Total	8361(100)	7949(100)	6958(100)	7017(100)	1610(100)	1557(100)

general equations of the best-fitted line for the isolated and non-isolated galaxies are respectively given by

$$\log_{10}(\text{SFR}) = 0.79 \pm 0.06 \log_{10}(M_{\star}) - 8.38 \pm 0.52, \quad (14)$$

$$\log_{10}(\text{SFR}) = 0.81 \pm 0.04 \log_{10}(M_{\star}) - 8.57 \pm 0.34, \quad (15)$$

where the associated errors are standard deviations in the slope and intercept. Table III indicates the number of galaxies with respect to the MS along with the percentage for the isolated and non-isolated galaxies above MS, within MS and below MS for SF (columns 2 and 3), strong AGN (columns 4 and 5), weak AGN (columns 6 and 7) galaxies, respectively.

The position of galaxies on the colour against the stellar mass diagram is shown in Fig. 6 for the SF, strong AGN, and weak AGN galaxies respectively. A already stated the width of the GV is given by Eqs. (12) and (13), representing the upper and lower lines, respectively. Table IV indicates the positioning of galaxies with respect to the GV with its percentage for isolated and non-isolated galaxies for the quenching sample above GV, within GV and below GV for SF (columns 2 and 3), strong AGN (columns 4 and 5), weak AGN (columns 6 and 7) galaxies, respectively. Table V indicates the Chi-square P-values between isolated and non-isolated galaxies above MS, within MS and below MS for SF (column 2), strong AGN (column 3), weak AGN (column 4) ageing galaxies, respectively and SF (column 5), strong AGN (column 6), weak AGN (column 7) quenching galaxies, respectively. Table VI indicates the Chi-square P-values between isolated and non-isolated galaxies above GV, within GV and below GV for SF (column 2), strong AGN (column 3), weak AGN (column 4) ageing galaxies, respectively and SF (column 5), strong AGN (column 6), weak AGN (column 7) quenching galaxies, respectively. These tables are used to trace how the positioning of galaxies with respect to MS and GV are affected by changing the galaxies' environment and the influence of nuclear activity on the relation.

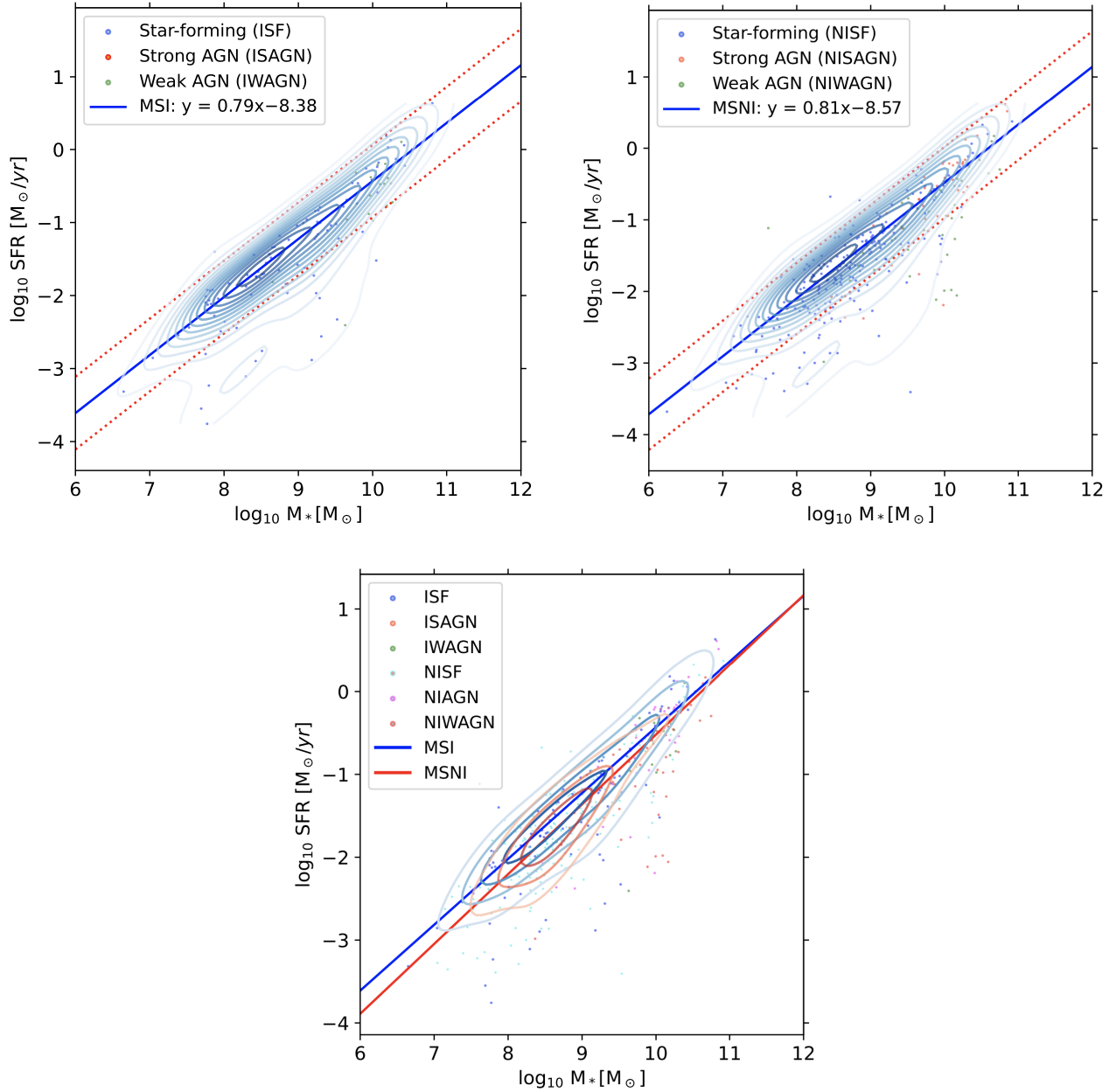


FIG. 5. Star formation main sequence (MS) for quenching galaxies: isolated sample (top left panel), non-isolated sample (top right panel), isolated and non-isolated on the same plot (bottom panel). In plots, MSI and MSNI denote the equations of the main sequence for isolated and non-isolated galaxies, respectively.

V. DISCUSSION

From Fig. 1, it is observed that the number of star-forming galaxies decreases by $\sim 12\%$ between isolated and non-isolated environments, while the retired galaxies increase by $\sim 14\%$, the number of strong AGN decreases by $\sim 3\%$ and the weak AGN increase by $\sim 1\%$. This indicates that the star-forming and retired galaxies are more significantly affected by the environment than the AGNs, hence environmental dependence is influenced by the presence of AGN sources. From Fig. 2 it is observed that the ageing galaxies decrease by $\sim 14\%$, while the retired galaxies increase by $\sim 14\%$. The undetermined galaxies decrease by $\sim 0.2\%$ while quenched galaxies increase by $\sim 0.3\%$ between isolated and non-isolated environments. This proves the scenario of Fig. 1, where the ageing (which mostly contains star-forming galaxies, see Ref. [19]) and retired galaxies are strongly affected by the environment than undetermined and quenched galaxies. This trend shows that quenched and retired galaxies are found in non-isolated environments rather than isolated environments while ageing is primarily found in isolated rather than non-isolated

TABLE III. Number of galaxies within (MS), above (Above MS), and below (Below MS) the star-forming main sequence for isolated (I) and non-isolated (NI) environments for the quenching transition (QGT) volume-limited sample.

Position (1)	Star-forming (%)		Strong AGN (%)		Weak AGN (%)	
	I (2)	NI (3)	I (4)	NI (5)	I (6)	NI (7)
MS	78(82.98)	158(76.33)	17(77.27)	25(69.44)	16(94.12%)	32(74.42)
Above MS	4(4.26)	23(11.11)	2(9.09)	7(19.44)	0(0)	1(2.33)
Below MS	12(12.77)	26(12.56)	3(13.64)	4(11.11)	1(5.88%)	10(23.26)
Total	94(100)	207(100)	22(100)	36(100)	17(100)	43(100)

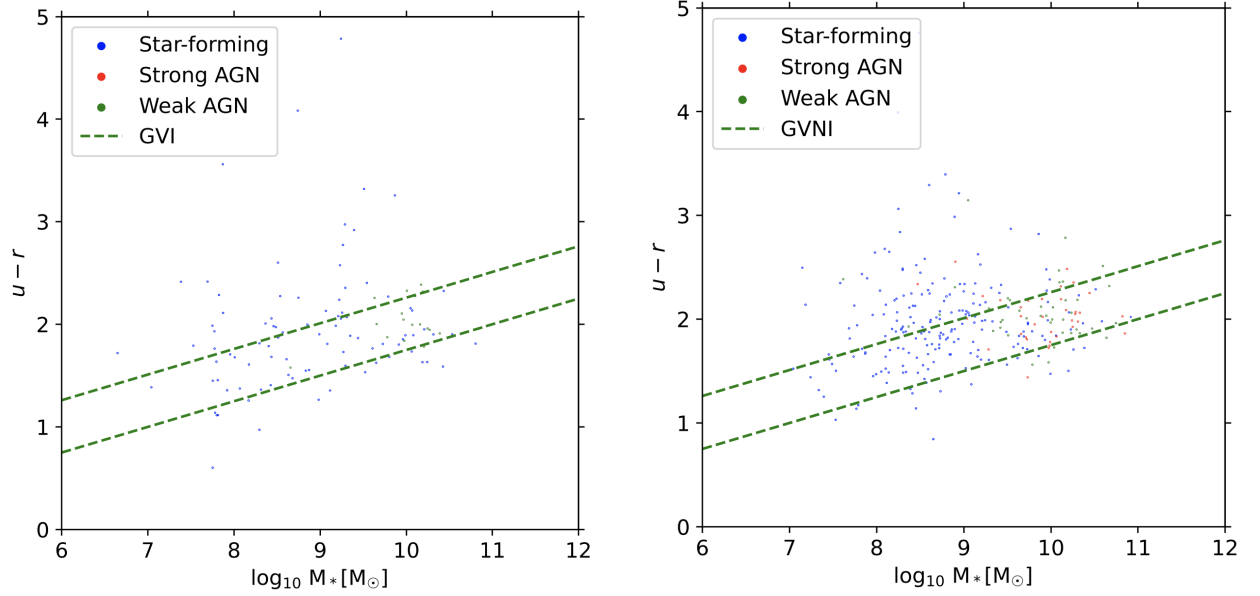


FIG. 6. Quenching galaxies' $u - r$ colour against stellar mass diagrams for the isolated (left panel) and non-isolated (right panel) samples. Here, GVI and GVNI denote the green valleys for isolated and non-isolated galaxies, respectively.

TABLE IV. Number of galaxies within the green valley (GV), above the green valley (Above GV) and below the green valley (Below GV) for isolated (I) and non-isolated (NI) galaxies in the quenching sample.

Position (1)	Star-forming (%)		Strong AGN (%)		Weak AGN (%)	
	I (2)	NI (3)	I (4)	NI (5)	I (6)	NI (7)
GV	42(44.68)	95(45.89)	13(59.09)	24(66.67)	12(70.59%)	25(58.14)
Above GV	36(38.30)	95(45.89)	2(9.09)	8(22.22)	4(23.53%)	14(32.56)
Below GV	16(17.02)	17(8.21)	7(31.82)	4(11.11)	1(5.88%)	4(9.30)
Total	94(100)	207(100)	22(100)	36(100)	17(100)	43(100)

environments. The study agrees with Ref. [20] using the density approach that quenched galaxies are primarily found in dense while ageing galaxies are found in less dense environments.

From Fig. 3 and Eqs. (10) and (11), the difference of ~ 0.03 in slope and ~ 0.30 in intercept are observed between isolated and non-isolated environment for ageing galaxies. The differences in slope and intercept are greater than the errors in slopes (0.01) and intercept (0.14). Furthermore, these differences produce P-values of 5.190×10^{-5} , and 6.408×10^{-5} for the slope and intercept, respectively which are both far less than the standard P-value in statistics (0.05). These two facts indicate that there is a significant difference in slope and intercept between isolated and non-isolated environments for transition ageing galaxies.

TABLE V. Chi-square P-values for ageing and quenching transitions between isolated and non-isolated galaxies within MS, above MS, and below MS.

Position (1)	Ageing			Quenching		
	Star-forming (2)	Strong AGN (3)	Weak AGN (4)	Star-forming (5)	Strong AGN (6)	Weak AGN (7)
MS	0.018	0.350	1	0.087	0.495	0.633
Above MS	0.001	0.942	0.656	0.251	0.730	0.072
Below MS	0.014	0.401	0.657	1	1	0.006

TABLE VI. Chi-square P-values for ageing and quenching transitions between isolated and non-isolated galaxies within GV, above GV, and below GV.

Position (1)	Ageing			Quenching		
	Star-forming (2)	Strong AGN (3)	Weak AGN (4)	Star-forming (5)	Strong AGN (6)	Weak AGN (7)
GV	0	0.113	0.139	0.943	0.763	0.928
Above GV	0.038	0.492	0.540	0.269	0.354	0.830
Below GV	0	0.055	0.063	0.269	0.108	0.310

The steeper slope (0.63) and lower intercept (-6.28) of non-isolated galaxies when compared to isolated galaxies with slope of 0.60 and intercept of -5.99 in Fig. 3, indicates that environmental factors affect the decrease of SFR in relation to stellar mass in ageing galaxies. This increases the transition of blue cloud to red sequence shaping the observed colour-mass bi-modality in Fig. 4, which is more rapid in the non-isolated than the isolated environments. The observed difference is evident in Table II where the non-isolated galaxy fraction is higher than isolated. Combining the observations in both figures it is evident that the environment is responsible for the decrease of SFR and the galaxy transition on the colour-stellar mass diagram.

From Fig. 5 and Eqs. (14) and (15), the difference of 0.02 in slope and 0.19 in intercept are observed between isolated and non-isolated environment for quenching galaxies. The difference in slope and intercept are less than the errors in slopes (0.06, 0.04) and intercepts (0.52, 0.34). Furthermore, these differences produce P-values of 0.50, and 0.36 for the slope and intercept, respectively which are both greater than the standard P-value in statistics (0.05). These two facts indicate that there is no significant difference in slope and intercept between isolated and non-isolated environments for quenching galaxies.

From Tables I, II, III, and IV it is observed that the number of SF, strong AGN, and weak AGN with respect to the MS have different fractions for the isolated and non-isolated environments in both ageing and quenching galaxies. In this observation the study agrees with the findings by Ref. [39], that galaxies classified as MS, quiescent and passive exhibit different fractions across different environments. On the other hand, the study agrees with Ref. [20], that ageing and quenching galaxies are found in different environments.

From column (2) of Table V, it is observed that the chi-square (χ^2) P-value for the difference in numbers of ageing galaxies between isolated and non-isolated within MS, above MS, and below MS is smaller (~ 0.011 on average) than the threshold (0.05) while from column (3) and (4) of Table V, it is observed that the P-values are greater ($\sim 0.564, \sim 0.771$ on average) than the threshold (0.05). On the other hand from columns (5), (6), (7) of Table V, it is observed that the P-values are greater ($\sim 0.446, \sim 0.742, \sim 0.237$ on average) than the threshold. Based on these observations, the positioning of SF ageing galaxies along the MS is affected by the environment, while the AGNs are not affected by the environment. The positioning of quenching galaxies is not influenced by the environment and this trend does not depend on the nature of nuclear activities of a particular galaxy.

From column (2) of Table VI, it is observed that the chi-square (χ^2) P-value for the difference in numbers of ageing galaxies between isolated and non-isolated within MS, above MS, and below MS is smaller (~ 0.013 on average) than the threshold (0.05) while from columns (3) and (4) of Table VI, it is observed that the P-values are greater ($\sim 0.220, \sim 0.247$ on average) than the threshold. On the other hand from columns (5), (6), (7) of Table VI, it is observed that the P-values are greater ($\sim 0.494, \sim 0.408, \sim 0.689$ on average) than the threshold. All these observations imply that the positioning of SF ageing galaxies with respect to the GV is affected by the environment, while the AGNs are not affected by the environment. The positioning of quenching galaxies with respect to the GV is not influenced by the environment and again this trend is not affected by the nature of nuclear activities of a particular galaxy.

It is widely believed that environmental influence is a long-term process which takes a few billion years. Even mergers effects

do not happen soon after galaxies' merging event, the median delay is ~ 1.5 Gyr where the time scale varies over a long range [65]. Due to the time scale factor, ageing is expected to be favoured by the environment rather than quenching. For example, the study in Ref. [66] revealed that the quenching to depend on mass and not environment using the 17 galaxy cluster candidates from the Cosmic Evolution Survey (COSMOS) field. Using the Sims Implementing Metals and Blackholes in Astrophysics (SIMBA) cosmological simulation to find the relationship between galaxy merging (related to environment) and quenching, Ref. [67] observed that the distribution of time delay between merging and quenching events does not suggest any physical relationship with fast or slow quenching. SIMBA also predicts that a major merger will trigger starbursts but it is not related to quenching in fast or slow mode. Ref. [68], revealed that the effect of the environment on the galaxy quenching is not completely separated from the effect of mass on galaxy quenching. This implies that mass is the leading parameter in the quenching process [69–74].

All necessary procedures have been considered in the analysis remembering the existence of observational bias, selection effect and methodological limitations. These include the bias from SDSS fibre collision and incomplete sky coverage which exclude low luminosity galaxies in the dense region explained in Section II A. The creation of the volume limited sample assured the uniformity in luminosity which is the key aspect to minimize bias explained in Section II B. The use of the friends-of-friends method is subject to uncertainty especially on the selection of the linking length which may over-link or under-link the galaxies affecting the analysis as explained in Section III A. Lastly, the uncertainty due to statistical analysis in the measurements of galaxy properties also is another important area to address as explained in Section III B. All these have been taken into account to minimize errors which may otherwise significantly influence the results.

VI. SUMMARY AND CONCLUSION

This study aimed at investigating if the environment is among the factors affecting the slow decrease (ageing), and fast decrease (quenching) of SFR in galaxies and how the relationship is influenced by the nuclear activity of a particular galaxy at the transition stage. We used the friends-of-friends method (defined in Section III) to assign the volume-limited sample from SDSS DR 12 galaxies into isolated and non-isolated environments. From a flux-limited sample of SDSS DR12, we constructed the volume-limited sample of 136274 galaxies within $-22.5 \leq M_r \leq -20.5$ (mag), containing 58032 ($\sim 43\%$) isolated and 78233 ($\sim 57\%$) non-isolated galaxies. The galaxies were classified according to their nature of nuclear activity employing WHAN diagnostic diagrams (shown by Fig. 1) into star-forming, strong AGN, weak AGN, and retired galaxies aiming to investigate the influence of nuclear activity on the environmental dependence of galaxies. Ageing diagrams (shown by Fig. 2) were used to classify the galaxies into ageing, quenched, undermined, and retired galaxies. Since we aim to study the ageing and quenching galaxies in the transition stage, we used the $0.5 < (g - r) < 0.7$, criteria from Ref. [19], to obtain a total number of 33452 ageing, galaxies in transition stage (AGT) where 16929 are isolated and 16523 are non-isolated. Furthermore, a total number of 419 quenching (QGT) was obtained, where 133 are isolated and 286 are non-isolated. The AGT and QGT were used throughout the study to investigate the star formation main sequence and the colour stellar mass diagram for ageing galaxies (shown by Figs. 3 and 4) and quenching galaxies (shown by Figs. 5 and 6). The following significant findings are revealed via this study:

- Ageing galaxies are mostly found in isolated rather than the non-isolated environment while quenching galaxies are found in non-isolated rather than the isolated environment.
- The significant change in slope and intercept of the equation of star formation main sequence by 0.03 dex, 0.30 dex respectively between isolated and non-isolated environments for ageing galaxies was observed indicating that the slope and intercept of ageing star formation main sequence are influenced by the environment.
- The insignificant change in slope and intercept of the equation of star formation main sequence by 0.02 dex, 0.12 dex respectively between isolated and non-isolated environments for quenching galaxies was observed indicating that the slope and intercept of quenching star formation main sequence are not influenced by the environment.
- A significant change in the number of ageing SF galaxies above, within and below the main sequence, similarly above, within and below the green valley between isolated and non-isolated environments was observed indicating that the positioning of ageing star forming galaxies with respect to the main sequence and the green valley is influenced by the environment. On the other hand insignificant change in the number of ageing strong and weak AGN was observed indicating that the positioning of ageing AGN are not influenced by the environment. This implies that ageing depends on the environment and this relationship is influenced the nuclear activity.
- An insignificant change in the number of quenching SF, strong AGN, and weak AGN was observed above, within and below the main sequence, similarly above, within and below the green valley between isolated and non-isolated environments was observed indicating that the positioning of quenching star forming galaxies with respect to the main sequence and the

green valley are not influenced by the environment and the nuclear activity have negligible influence on the independence of quenching on the environment.

Altogether, the results of this study help us to understand galaxy evolution by revealing how environmental factors and nuclear activity affect the galaxy's transitions. The significant environmental dependence of ageing proves the results from theoretical predictions on the role of environmentally driven processes such as the ram pressure stripping able to remove the gas reservoir, leading to strangulation or starvation (the suppression of gas infall or galaxy interactions) in the star formation rate of galaxies. The independence of quenching on the environment proves that internally triggered mechanisms such as negative feedback from AGNs, supernovae winds or the stabilisation of the gas against fragmentation lead to the rule on the quenching process. The difference in slopes and intercepts between ageing and quenching proves that the process of galaxy evolution is not uniform but a multi-process indicating the combination of both environmental and internal factors. The results challenge the oversimplified notion and highlight the interplay between environment, internal galaxy dynamics, and nuclear activity.

Despite the strength of using the volume limited sample and the effectiveness of using the WHAN diagnostic diagram in galaxy classification to minimize the selection bias these obviously may exclude some populations such as faint, massive and composite galaxies. Furthermore, comparing two populations of isolated and non-isolated galaxies may exclude the intermediate density environment galaxies which may not significantly change the implication of existing results but provide additional insights.

In the future, we will apply similar analysis on the galaxies of high redshift surveys example the James Webb Space Telescope (JWST) Ref. [75] to again characterize the influence of the environment on ageing and quenching of galaxies. Further, we plan to use integral field spectroscopy (IFS) surveys example Mapping Nearby Galaxies survey at APO (MaNGA) Ref. [76] data to investigate the role of morphology-environment relation on galaxy transitions.

ACKNOWLEDGEMENTS

PP acknowledges support from The Government of Tanzania through the India Embassy, Mbeya University of Science and Technology (MUST) for Funding and SDSS for providing data. UDG is thankful to the Inter-University Centre for Astronomy and Astrophysics (IUCAA), Pune, India for the Visiting Associateship of the institute. Funding for SDSS-III has been provided by the Alfred P. Sloan Foundation, the Participating Institutions, the National Science Foundation, and the U.S. Department of Energy Office of Science. The SDSS-III website is <http://www.sdss3.org/>. SDSS-III is managed by the Astrophysical Research Consortium for the Participating Institutions of the SDSS-III Collaboration including the University of Arizona, the Brazilian Participation Group, Brookhaven National Laboratory, Carnegie Mellon University, the University of Florida, the French Participation Group, the German Participation Group, Harvard University, the Instituto de Astrofísica de Canarias, the Michigan State/Notre Dame/JINA Participation Group, Johns Hopkins University, Lawrence Berkeley National Laboratory, Max Planck Institute for Astrophysics, Max Planck Institute for Extraterrestrial Physics, New Mexico State University, New York University, Ohio State University, Pennsylvania State University, University of Portsmouth, Princeton University, the Spanish Participation Group, University of Tokyo, the University of Utah, Vanderbilt University, the University of Virginia, the University of Washington, and Yale University.

-
- [1] G. Kauffmann, S. White, *The Environmental Dependence of the Relations between Stellar Mass, Structure, Star Formation and Nuclear Activity in Galaxies*, *MNRAS* **353**, 713 (2004) [[arXiv:astro-ph/0402030](#)].
 - [2] C. Tremonti, T. Heckman, *The Origin of the Mass–Metallicity Relation: Insights from 53,000 Star-Forming Galaxies in the SDSS*, *ApJ* **613**, 898 (2004) [[arXiv:astro-ph/0405537](#)].
 - [3] Y. Peng, S. Lilly, K. Kovač, M. Bolzonella, L. Pozzetti, et al., *Mass and Environment as Drivers of Galaxy Evolution in SDSS and zCOSMOS and the Origin of the Schechter Function*, *ApJ* **721**, 193 (2010) [[arXiv:1003.4747](#)].
 - [4] J. Brinchmann, S. Charlot, *The physical properties of star forming galaxies in the low redshift universe*, *MNRAS* **351**, 1151 (2004) [[arXiv:astro-ph/0311060](#)].
 - [5] T. Gonçalves, D. Martin, K. Menéndez-Delmestre, T. Wyder, et al., *Quenching star formation at intermediate redshifts: downsizing of the mass flux density in the green valley*, *ApJ* **759**, 67 (2012) [[arXiv:1209.4084](#)].
 - [6] J. Moustakas, A. Coil, J. Aird, M. Blanton, R. Cool, et al., *Constraints on Star Formation Quenching and Galaxy Merging, and the Evolution of the Stellar Mass Function From $z = 0 - 1$* , *ApJ* **767**, 50 (2013) [[arXiv:1301.1688](#)].
 - [7] D. Elbaz, E. Daddi, D. Borgne, *The reversal of the star formation-density relation in the distant universe*, *A&A* **468**, 33 (2007) [[arXiv:astro-ph/0703653](#)].
 - [8] J. Speagle, C. Steinhardt, P. Capak, J. Silverman, et al., *A Highly Consistent Framework for the Evolution of the Star-Forming "Main Sequence" from $z \sim 0 - 6$* , *ApJS* **214**, 15 (2014) [[arXiv:1405.2041](#)].
 - [9] S. Leslie, L. Kewley, D. Sanders, N. Lee, *Quenching star formation: insights from the local main sequence*, *MNRAS* **455**, L82 (2015) [[arXiv:1509.03632](#)].

- [10] E. Daddi, M. Dickinson, G. Morrison, R. Chary, et al., *Multiwavelength study of massive galaxies at $z \sim 2$. I. Star formation and galaxy growth*, **ApJ** **670**, 156 (2007). [arXiv:0705.2831].
- [11] T. Yuan, L. Kewley, D. Sanders, *The Role of Starburst-Active Galactic Nucleus Composites in Luminous Infrared Galaxy Mergers: Insights from the New Optical Classification Scheme*, **ApJ** **709**, 884 (2010).
- [12] J. Rich, L. Kewley, M. Dopita, *Galaxy-Wide Shocks in Late-Merger Stage Luminous Infrared Galaxies*, **ApJ** **782**, 9 (2014) [arXiv:1104.1177].
- [13] K. Schawinski, D. Thomas, M. Sarzi, C. Maraston, et al., *Observational evidence for AGN feedback in early-type galaxies*, **MNRAS** **382**, 1415 (2007) [arXiv:0709.3015].
- [14] K. Whitaker, P. Dokkum, G. Brammer, M. Franx, *The star formation mass sequence out to $z=2.5$* , **ApJL** **754**, L29 (2015) [arXiv:1205.0547].
- [15] T. Shimizu, R. Mushotzky, M. Meléndez, M. Koss, et al., *Decreased specific star formation rates in AGN host galaxies*, **MNRAS** **452**, 1841 (2007) [arXiv:1506.07039].
- [16] S. Faber, C. Willmer, C. Wolf, D. Koo, B. Weiner, J. Newman, et al., *Galaxy Luminosity Functions to $z \sim 1$: DEEP2 vs. COMBO-17 and Implications for Red Galaxy Formation*, **ApJ** **665**, 265 (2007) [arXiv:astro-ph/0506044].
- [17] R. Hickox, J. Mullaney, D. Alexander, C. Chen, F. Civanoet, al., *Black hole variability and the star formation–active galactic nucleus connection: do all star-forming galaxies host an active galactic nucleus*, **ApJ** **782**, 9 (2014) [arXiv:1306.3218].
- [18] K. Schawinski, C. Urry, B. Simmons, L. Fortson, S. Kaviraj, et al., *The green valley is a red herring: Galaxy Zoo reveals two evolutionary pathways towards quenching of star formation in early- and late-type galaxies*, **MNRAS** **440**, 889 (2014).
- [19] P. Corcho-Caballero, Y. Ascasibar, L. Cortese, S. Sanchez, et al., *Ageing and quenching through the Ageing Diagram – II. Physical characterization of galaxies*, **MNRAS** **524**, 3692 (2023) [arXiv:2307.02024].
- [20] P. Corcho-Caballero, Y. Ascasibar, S. Sanchez, Á. López-Sánchez, *Ageing and quenching through the ageing diagram: predictions from simulations and observational constraints*, **MNRAS** **520**, 193 (2023) [arXiv:2208.14084].
- [21] A. Fitts, M. Boylan-Kolchin, O. Elbert, J. Bullock, et al., *Fire in the field: simulating the threshold of galaxy formation*, **MNRAS** **471**, 3547 (2017).
- [22] J. Gensior, J. Kruijssen, B. Keller, *Heart of darkness: the influence of galactic dynamics on quenching star formation in galaxy spheroids*, **MNRAS** **495**, 199 (2020).
- [23] L. Cortese, B. Catinella, R. Smith, *The Dawes Review 9: The role of cold gas stripping on the star formation quenching of satellite galaxies*, **PASA** **38**, e035 (2021).
- [24] T. Brown, B. Catinella, L. Cortese, C. Lagos, et al., *Cold gas stripping in satellite galaxies: from pairs to clusters*, **MNRAS** **466**, 1275 (2017).
- [25] M. Thorp, S. Ellison, H. Pan, L. Lin, et al., *The ALMaQUEST Survey X: what powers merger induced star formation?*, **ApJ** **516**, 1462 (2022).
- [26] H. Akims, D. Narayanan, K. Whitaker, R. Davé, et al., *Quenching and the UVJ Diagram in the SIMBA Cosmological Simulation*, **ApJ** **929**, 94 (2022).
- [27] S. Tacchella, C. Conroy, S. Faber, B. Johnson, et al., *Fast, slow, early, late: quenching massive galaxies at $z \sim 0.8$* , **ApJ** **926**, 134 (2022).
- [28] K. Suess, M. Kriek, R. Bezanson, J. Greene, et al., *Studying Quenching in Intermediate- z Galaxies—Gas, Momentum, and Evolution*, **ApJ** **926**, 86 (2022).
- [29] F. Belfiore, R. Maiolino, K. Bundy, K. Masters, et al., *SDSS IV MaNGA – $sSFR$ profiles and the slow quenching of discs in green valley galaxies*, **MNRAS** **477**, 3014 (2018).
- [30] N. Abdurro’uf, K. Accetta, C. Aerts, V. Silva, et al., *The Seventeenth Data Release of the Sloan Digital Sky Surveys: Complete Release of MaNGA, MaStar, and APOGEE-2 Data*, **ApJ** **259**, 2 (2022).
- [31] G. Erfanianfar, P. Popesso, A. Finoguenov, D. Wilman, et al., *Non-linearity and environmental dependence of the star-forming galaxies main sequence*, **MNRAS** **455**, 2839 (2016) [arXiv:1511.01899].
- [32] P. Lang, S. Wuyts, R. Somerville, N. Schreiber, R. Genzel, et al., *Bulge Growth and Quenching since $z = 2.5$ in CANDELS/3D-HST*, **ApJ** **788**, 788 (2014) [arXiv:1402.0866].
- [33] A. Bluck, L. Maiolino, S. Sánchez, F. Sebastian, L. Sara, et al., *Are galactic star formation and quenching governed by local, global, or environmental phenomena?*, **MNRAS** **492**, 96 (2020).
- [34] J. Leja, S. Joshua, Y. Speagle, T. Benjamin, D. Johnson, et al., *A New Census of the $0.2 < z < 3.0$ Universe. II. The Star-forming Sequence*, **ApJ** **936**, 165 (2022).
- [35] J. Thorne, A. Robotham, L. Davies, S. Bellstedt, et al., *Deep Extragalactic Visible Legacy Survey (DEVILS): SED fitting in the D10-COSMOS field and the evolution of the stellar mass function and $SFR-M_\star$ relation*, **MNRAS** **505**, 540 (2021).
- [36] S. Leslie, E. Schinnerer, D. Liu, B. Magnelli, et al., *The VLA-COSMOS 3 GHz Large Project: Evolution of Specific Star Formation Rates out to $z \sim 5$* , **ApJ** **899**, 58 (2020).
- [37] D. Croton, V. Springel, S. White, G. Lucia, et al., *The many lives of active galactic nuclei: cooling flows, black holes and the luminosities and colours of galaxies*, **MNRAS** **365**, 11 (2013) [arXiv:astro-ph/0508046].
- [38] D. Rosario, P. Santini, D. Lutz, L. Shao, et al., *The mean star formation rate of X-ray selected active galaxies and its evolution from $z \sim 2.5$: results from PEP-Herschel*, **A&A** **545**, A45 (2012) [arXiv:1203.6069].
- [39] A. Oemler, L. Abramson, M. Gladders, A. Dressler, et al., *The Star Formation Histories of Disk Galaxies: The Live, the Dead, and the Undead*, **ApJ** **844**, 45 (2017).
- [40] S. Croom, J. Lawrence, J. Bland-Hawthorn, J. Bryant et al., *The Sydney-AAO multi-object integral field spectrograph*, **MNRAS** **421**, 872 (2012).
- [41] J. Bryant, M. Owers, A. Robotham, S. Croom, et al., *The SAMI Galaxy Survey: instrument specification and target selection*, **MNRAS** **447**, 2857 (2005).

- [42] E. Tempel, T. Tuvikene, *Merging groups and clusters of galaxies from the SDSS data. The catalogue of groups and potentially merging systems*, **A&A** **602**, A100 (2017) [arXiv:1704.04477].
- [43] P. Ade, N. Aghanim, *Planck 2015 results. XXIII. The thermal Sunyaev-Zeldovich effect–cosmic infrared background correlation*, **A&A** **594**, A23 (2016) [arXiv:1509.06555].
- [44] D. Eisenstein, D. Weinberg, *SDSS-III: Massive spectroscopic surveys of the distant universe, the Milky Way, and extra-solar planetary systems*, **AJ** **142**, 72 (2011) [arXiv:1101.1529].
- [45] S. Alam, F. Albareti, C. Prieto, *The Eleventh and Twelfth Data Releases of the Sloan Digital Sky Survey: Final Data from SDSS-III*, **ApJS** **219**, 12 (2015) [arXiv:1501.00963].
- [46] D. Schlegel, D. Finkbeiner, M. Davis, *Maps of dust infrared emission for use in estimation of reddening and cosmic microwave background radiation foregrounds*, **ApJ** **500**, 525 (1998).
- [47] M. Strauss, D. Weinberg, R. Lupton, V. Narayanan, et al., *Spectroscopic target selection in the Sloan Digital Sky Survey: the main galaxy sample*, **AJ** **124**, 3 (2002).
- [48] M. Blanton, S. Roweis, *K-corrections and filter transformations in the ultraviolet, optical, and near-infrared*, **AJ** **133**, 734 (2007) [arXiv:astro-ph/0606170].
- [49] M. Blanton, D. Hogg, N. Bahcall, J. Brinkmann, et al., *The galaxy luminosity function and luminosity density at redshift $z = 0.1$* , **AJ** **592**, 819 (2003) [arXiv:astro-ph/0210215].
- [50] E. Tempel, E. Tago, L. Liivamägi, *Groups and clusters of galaxies in the SDSS DR8-Value-added catalogues*, **A&A** **540**, A106 (2012) [arXiv:1112.4648].
- [51] E. Tempel, A. Tamm, M. Gramann, *Flux- and volume-limited groups/clusters for the SDSS galaxies: catalogues and mass estimation*, **A&A** **566**, A1 (2014) [arXiv:1402.1350].
- [52] N. Ball, J. Loveday, R. Brunner, I. Baldry, J. Brinkmann, et al., *Bivariate galaxy luminosity functions in the Sloan Digital Sky Survey*, **MNRAS** **373**, 845 (2006).
- [53] P. Schechter, *An analytic expression for the luminosity function for galaxies*, **ApJ** **203**, 297 (1976).
- [54] X. Deng, Y. Xin, P. Wu, P. Jiang, et al., *Some Properties of Active Galactic Nuclei in the Volume-limited Main Galaxy Samples of SDSS DR8*, **ApJ** **754**, 82 (2012).
- [55] C. Kennicutt, *Star Formation in Galaxies Along the Hubble Sequence*, **A&A** **39**, 189 (1998) [arXiv:astro-ph/9807187].
- [56] S. Salim, J. Lee, R. Davé, *On the Mass-Metallicity-Star Formation Rate Relation for Galaxies at $z \sim 2$* , **ApJ** **808**, 14pp (2015) [arXiv:1506.03080].
- [57] S. Sanchez, V. Avila-Reese, H. Hernandez-Toledo, E. Cortes-Suarez, et al., *SSDSS IV MaNGA - Properties of AGN host galaxies*, **RxMAA** **54**, 1 (2018).
- [58] R. Cid-Fernandes, G. Stasinska, A. Mateus, N. Vale-Asari, *A comprehensive classification of galaxies in the Sloan Digital Sky Survey: how to tell true from fake AGN*, **MNRAS** **413**, 1687 (2011).
- [59] L. Kewley, B. Groves, G. Kauffmann, T. Heckman, et al., *The host galaxies and classification of active galactic nuclei*, **MNRAS** **372**, 961 (2006) [arXiv:astro-ph/0605681].
- [60] G. Kauffmann, T. Heckman, C. Tremonti, J. Brinchmann, et al., *The host galaxies of active galactic nuclei*, **MNRAS** **346**, 1055 (2003) [arXiv:astro-ph/0304239].
- [61] L. Kewley, M. Dopita, R. Sutherland, C. Heisler, et al., *Theoretical modeling of starburst galaxies*, **ApJ** **556**, 121 (2001) [arXiv:astro-ph/0106324].
- [62] R. Singh, G. van de Ven, K. Jahnke, M. Lyubenova, et al., *The nature of LINER galaxies*, **A&A** **558**, A43 (2013).
- [63] L. Sánchez, *Spatially Resolved Spectroscopic Properties of Low-Redshift Star-Forming Galaxies*, **ARA&A** **99**, 58 (2020) [arXiv:1911.06925].
- [64] L. Sánchez, C. Walcher, C. Lopez-Cobá, J. Barrera-Ballesteros, *From Global to Spatially Resolved in Low-Redshift Galaxies*, **RxMAA** **57**, 3 (2021) [arXiv:2009.00424].
- [65] Y. Peng, R. Maiolino, R. Cochrane, *Strangulation as the primary mechanism for shutting down star formation in galaxies*, **Nature** **521**, 192 (2015) [arXiv:1505.03143].
- [66] Z. Mao, T. Kodama, J. Pérez-Martínez, T. Suzuki, et al., *Revealing impacts of stellar mass and environment on galaxy quenching*, **A&A** **666**, A141 (2022) [arXiv:2208.00722].
- [67] F. Rodríguez-Montero, R. Davé, V. Wild, D. Anglés-Alcázar, et al., *Mergers, starbursts, and quenching in the simba simulation*, **MNRAS** **490**, 2139 (2019) [arXiv:1907.12680].
- [68] V. Tan, A. Muzzin, Z. Marsan, V. Sok, et al., *Resolved Stellar Mass Maps of Galaxies in the Hubble Frontier Fields: Evidence for Mass Dependency in Environmental Quenching*, **ApJ** **933**, 30 (2022) [arXiv:2205.0791].
- [69] X. Ge, F. Liu, Q. Gu, E. Contini, et al., *Conditions for galaxy quenching at $0.5 < z < 2.5$ from CANDELS: compact cores and environment*, **RAA** **20**, 116 (2022).
- [70] A. Reeves, M. Balogh, R. Van der Burg, A. Finoguenov, et al., *The GOGREEN survey: dependence of galaxy properties on halo mass at $z > 1$ and implications for environmental quenching*, **MNRAS** **506**, 3364 (2021) [arXiv:2107.03425].
- [71] P. Corcho-Caballero, J. Casado, Y. Ascasibar, R. García-Benito, et al., *Galaxy evolution on resolved scales: ageing and quenching in CALIFA*, **MNRAS** **507**, 5477 (2021) [arXiv:2107.13478].
- [72] F. Hasan, J. Burchett, A. Abeyta, D. Hellinger, et al., *The Evolving Effect of Cosmic Web Environment on Galaxy Quenching*, **MNRAS** **950**, 114 (2023) [arXiv:2303.08088].
- [73] R. Kipper, A. Tamm, E. Tempel, R. Propris, et al., *The role of stochastic and smooth processes in regulating galaxy quenching*, **A&A** **647**, A32 (2021) [arXiv:2101.08549].
- [74] M. Einasto, R. Kipper, P. Tenjes, J. Einasto, et al., *Death at watersheds: Galaxy quenching in low-density environments*, **A&A** **668**, A69 (2022). [arXiv:2210.10761].

- [75] M. McElwain, L. Feinberg, M. Perrin, M. Clampin, et al., *The James Webb Space Telescope Mission: Optical Telescope Element Design, Development, and Performance*, **PASP** **135**, 058001 (2023). [[arXiv:2301.01779](#)].
- [76] N. Drory, N. MacDonald, M.A. Bershad, K. Bundy, et al., *The MaNGA integral field unit fiber feed system for the Sloan 2.5 m telescope*, **AJ** **149**, 77 (2015) [[arXiv:1412.1535](#)].